A Framework for the Symmetric Generalisation of the Miura-ori

Pooya Sareh* and Simon D. Guest

University of Cambridge, UK

(Submitted on 6/11/2014, Reception of revised paper 29/05/2015, Accepted on 23/06/2015)

ABSTRACT: The Miura fold pattern, or the Miura-ori, is a flat-foldable origami tessellation which has been applied to the folding of deployable structures for various engineering and architectural applications. In recent years, researchers have proposed systematic (see, e.g., [1] or [2]), and also free-form [3], variations on the Miura pattern.

This paper develops a geometric framework for the symmetric generalisation of the Miura-ori while preserving the 'stacking while folding' behaviour of the pattern. We present a number of novel concepts and definitions which help us apply systematic variations on the original pattern. We study the Miura crease pattern as a *pmg* wallpaper pattern which is one of the seventeen distinct wallpaper groups. We reduce the symmetry of the Miura-ori to obtain new patterns while preserving the flat-foldability condition at each node. We conclude that we are able to use the Miura-ori, which is a globally planar pattern in its partially folded states, to systematically design either 'globally planar' or 'globally curved' patterns, through appropriate design variations on the original pattern.

1. INTRODUCTION

The Miura-ori [4], is a flat-foldable origami tessellation which has been applied to the folding of structures for use in various engineering and architectural applications. A polypropylene model of the Miura-ori in three different folding states is depicted in Figure 1. The Miura-ori is considered to be a functional pattern for the design of foldable objects. Example applications are shown in Figure 2.

In this paper, we will study the Miura fold pattern from a symmetry perspective. In particular, we shall consider an infinite repetitive pattern which has 'plane' or wallpaper symmetry. Mathematicians have shown (see, e.g., [7]) that there are exactly seventeen distinct *plane symmetry groups*, also known as *wallpaper groups* or *plane crystallographic groups*. Each group has a unique *unit cell*, and a certain number of *symmetry elements*, placed in certain positions relative to the unit cell. The symmetry elements include centres of *rotation*, axes of *reflection*, and axes of *glide reflection*. Schattschneider [8] presents the 'international notation' for the seventeen plane symmetry groups that we use here. Further details of the plane symmetry groups are presented in the International Tables for Crystallography [9].

This paper develops a framework for the symmetric generalisation of the Miura-ori while preserving the 'stacking while folding' behaviour of the pattern. It discusses the Miura fold pattern and some systematic variations on it from a plane symmetry perspective. There are two general assumptions we use throughout this study:

i. We consider a crease pattern to be a set of 'directionless' creases. In other words, the 'fold direction' or 'mountain-valley assignment' of the fold lines does not affect the symmetry of a pattern. This assumption allows us to explore a wider range of crease patterns, and obtain

*Corresponding author e-mail: p.sareh@imperial.ac.uk

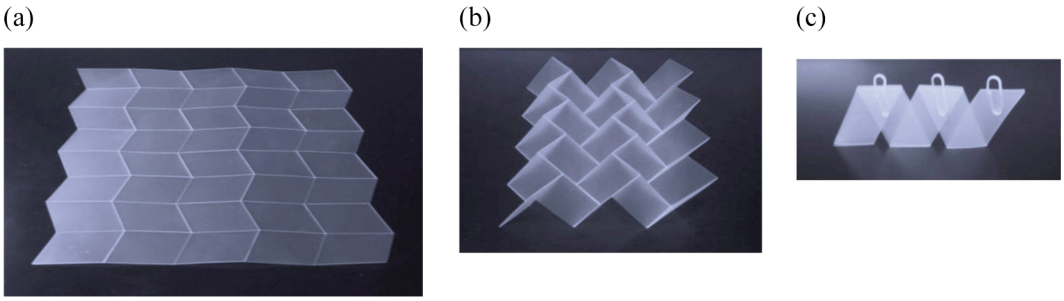

Figure 1. A polypropylene model for the Miura-ori in three different folding states: (a) developed; (b) partially folded; (c) flat-folded (kept flat-folded using paper clips).

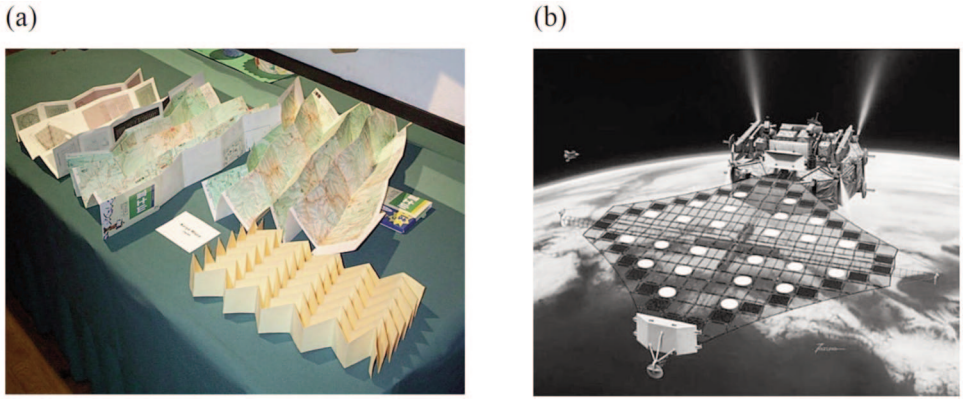

Figure 2. (a) Maps folded based on the Miura-ori [5]; (b) deployable solar cell array based on the Miura-ori [6].

symmetric fold patterns which would not be achievable without it. The 'mountain-valley' assignment of fold lines will be made after the generation of the directionless crease pattern.

ii. Two crease patterns are considered to be 'similar' if a uniform scaling or rigid motion of one of them can make it coincide with the other one.

In the next section, the symmetry of the Miura-ori is investigated.

2. SYMMETRY OF THE MIURA FOLD PATTERN

The symmetry of an infinitely repeated Miura crease pattern is *pmg* in the international notation. For a typical Miura-ori crease pattern shown in Figure 3, the 'starting parallelogram' of the pattern, P, from which the entire pattern can be generated by symmetry operations, is shaded in green. It has an acute angle α, and two side lengths b and l, where b is along the horizontal lines of the pattern, i.e. along the y-direction.

Every wallpaper pattern has a finite region called a 'unit cell' which repeats under the action of two linearly independent translations. Four choices for the smallest *pmg* unit cell for the Miura-ori are shown in Figure 3. The blue shaded area shows the 'fundamental region' of the pattern. A fundamental region is a minimal part of a pattern that generates the entire pattern under the action of all the symmetry operators which exist in the pattern [10]. Different colours for a symmetry element represent different classes of that element in the pattern. There are two different choices for the unit cell which both match the standard *pmg* unit cell used in the International Tables for Crystallography [9]. These two unit cells are shown on the left part of the figure. We primarily use the unit cell shown on the top-left along with its axes, throughout this work. We call this the *primary standard* choice for the smallest unit cell of the Miuraori. However, in order to cover a wider range of variations, it is sometimes necessary to consider an *alternative standard* choice for the smallest unit cell of the Miura-ori, which is marked by a '+' symbol. There are also two non-standard unit cells shown on the right hand side of the figure. We call the upper unit cell the *primary non-standard* choice, and the lower unit cell the *alternative non-standard* choice, marked by a '+' symbol. Note that the entire pattern can be generated from a unit cell by only translations. The translation vectors of the pattern in the x- and y-directions are shown as **a** and **b**, respectively. We define a *unit fragment* of a repetitive mesh as a collection of adjacent facets which generate the entire pattern using the translation vectors of the pattern. The unit fragment of the Miura fold pattern, as depicted on the

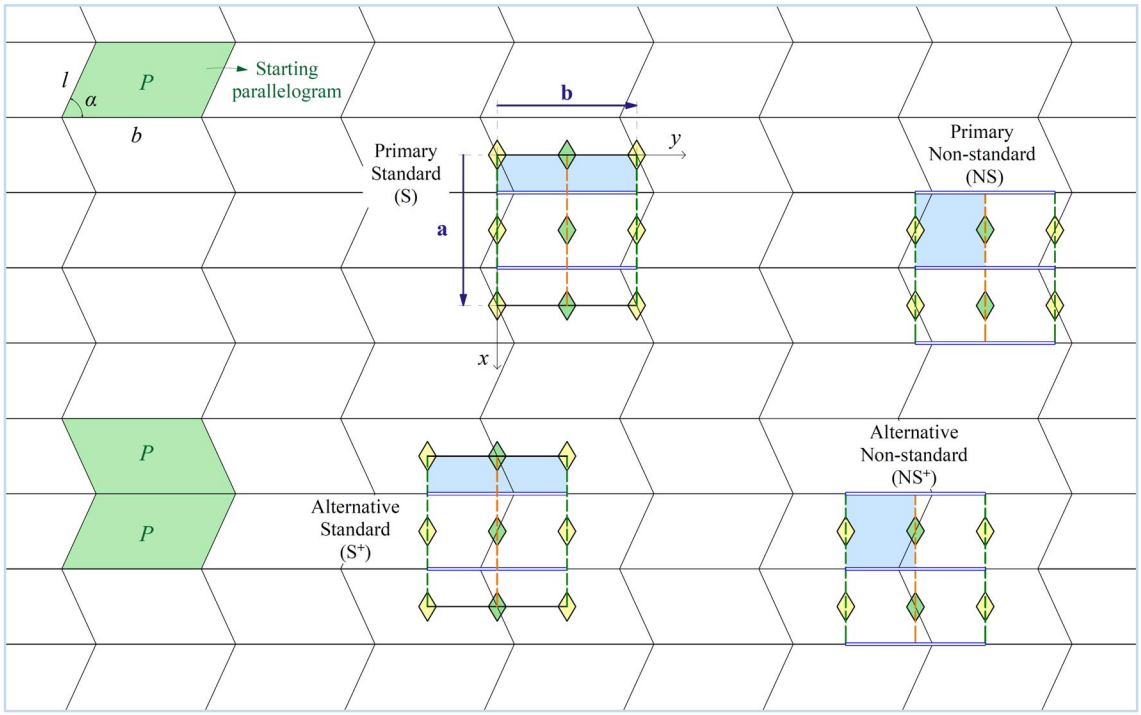

Figure 3. Four choices for the smallest *pmg* unit cell for the Miura-ori. Double and dashed lines represent reflection and glide reflection axes, respectively. 2-fold axes are shown by rhombuses. The blue shaded area shows the fundamental region of the pattern. The starting parallelogram of the pattern is shaded in green.

bottom left of Figure 3, consists of a pair of starting parallelograms which share a fold line on the horizontal lines of the pattern, i.e. along the *y*-direction.

2.1. Recomposition of a unit cell

We can recompose the unit cell of a repetitive mesh to obtain its unit fragment. From Figure 4 we can see that the smallest unit cell of the Miura-ori contains two parallelograms. The left hand section of this figure shows how to move the triangular fragments (bordered by bold lines) formed by the crease lines and the borders of the unit cell to obtain the figure in the middle; it is then sufficient to translate the bordered parallelogram on the bottom of the middle figure in the opposite *x*-direction to form two complete parallelograms. We use this recomposition process to find out the number of quadrilaterals within the unit cell of a crease pattern throughout this study.

The recomposition process gives us the number of quadrilaterals 'in each direction' in the unit cell of a pattern. As Figure 4 shows, the smallest unit cell for the Miura-ori contains two parallelograms in the *x*-direction and one parallelogram in the *y*-direction. We call this crease pattern a $pmg_{2,1}$ pattern. We classify the crease patterns obtained by applying variations on the Miura fold pattern using the following definition:

***Definition* 1:** A repetitive convex quadrilateral mesh designed by displacing the nodes of the Miura fold pattern is called G_{ij}, where G is the name of its

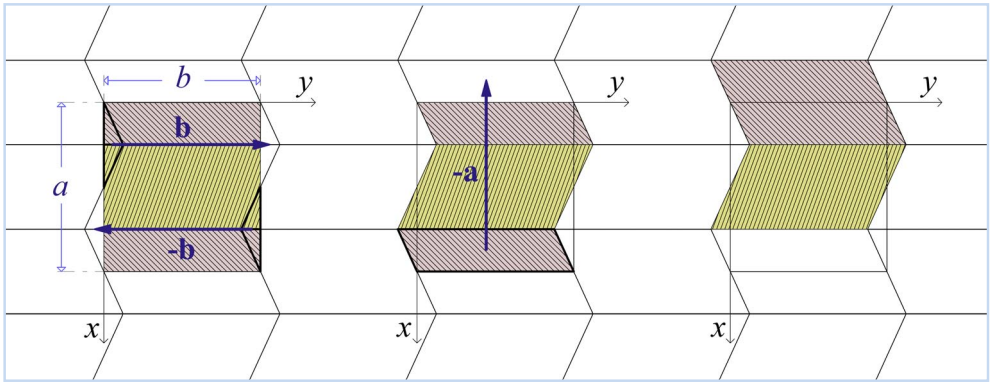

Figure 4. Recomposition of the Miura-ori unit cell to form its unit fragment.

maximal plane symmetry group, and i and j are the number of quadrilaterals in the x- and y-directions, respectively, within the unit cell of the pattern. The y-direction is the direction of the parallel fold lines in the Miura fold pattern before applying variations. Variations of the Miura-ori which can only be designed based on the alternative unit cells (shown in Figure 3) are denoted by G^{+}_{ij}.

We use this definition throughout this study. In the next section, we study the folding process of the Miura-ori from a symmetry viewpoint.

2.2. Transformation of the symmetry group through folding

This section explores symmetry in the folded configuration of the pattern. Consider a Miura fold pattern in the x-y plane, as shown on the left hand side of Figure 5. As discussed earlier, this pattern is $pmg_{2,1}$. Through the folding process, the pattern transforms from a 2D pattern in the x-y plane, infinite in two directions (x and y), into a 2D pattern in the y-z plane, infinite in one direction, y, and finite in the other one, z. The folded state is depicted on the right side of the figure.

The left hand side of Figure 6 shows the unit cell of a Miura-ori in the x-y plane, i.e. $pmg_{2,1}$, already shown in Figure 3. On the right, the unit cell of the folded state of the pattern, which lies in the y-z plane, is illustrated. It is a *p2mg* frieze pattern, containing a 2-fold axis, a mirror line, and a glide reflection line. Its short name is *mg* [11, 12]. For both unit cells, nodes with black labels represent the nodes associated with the fundamental region (the blue shaded area), while the grey nodes indicate their equivalents associated with the rest of the illustrated unit cell.

For the unit cell of the folded pattern, i.e. the frieze pattern, the unit cell has a translation vector $\mathbf{b}_f$ in the y-direction, and a height c_f in the z-direction, where index f denotes 'folded'. The blue shaded area shows the fundamental region of the pattern; all graphical

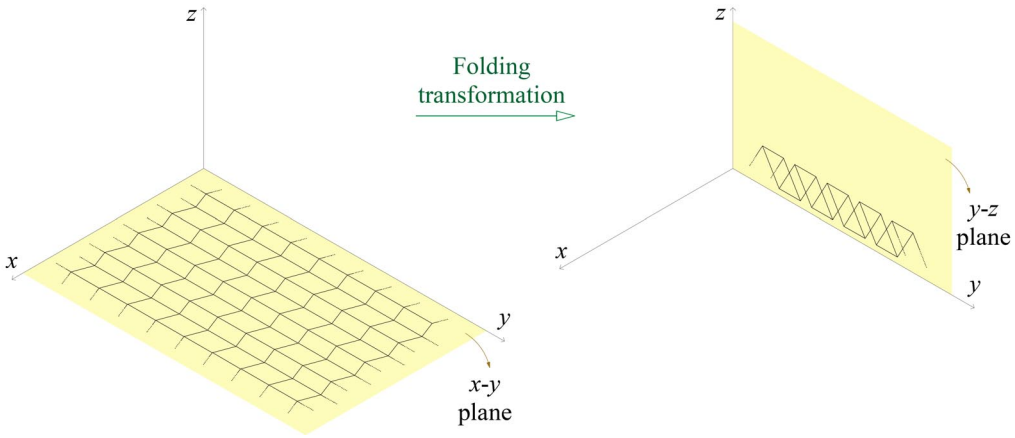

Figure 5. Transformation of a Miura-ori from a wallpaper pattern in the x-y plane into a frieze pattern in the y-z plane through the folding process.

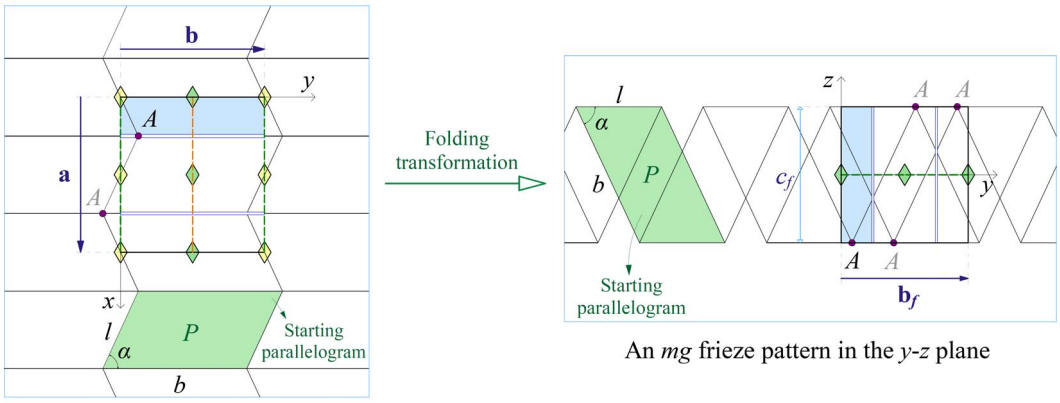

Figure 6. Left: the unit cell of a Miura fold pattern in the x-y plane; right: the unit cell of the folded state of the pattern, which lies in the y-z plane.

elements have the same meaning as in the wallpaper pattern. The following relationships exist between the dimensions of the unit cell and the geometry of the starting parallelogram:

$$b_f = 2b \cos \alpha \quad (1)$$

$$c_f = b \sin \alpha \quad (2)$$

The particular Miura-ori shown in Figure 6 is an infinite pattern, a wallpaper pattern, which folds to another infinite pattern, a frieze pattern. Some variations of the Miura fold pattern also possess this property. The following definition is proposed for these types of variations of the Miura-ori:

***Definition* 2:** A tessellating variation of the Miura-ori is called *globally planar* if it folds to either a frieze pattern, or a wallpaper pattern, in its flat state.

An example for a variation of the Miura-ori which folds to a wallpaper pattern is the inclined variation [2] shown in Figure 8.b. The unit cell and unit fragment of this fold pattern are illustrated in Figure 7.a. The unit

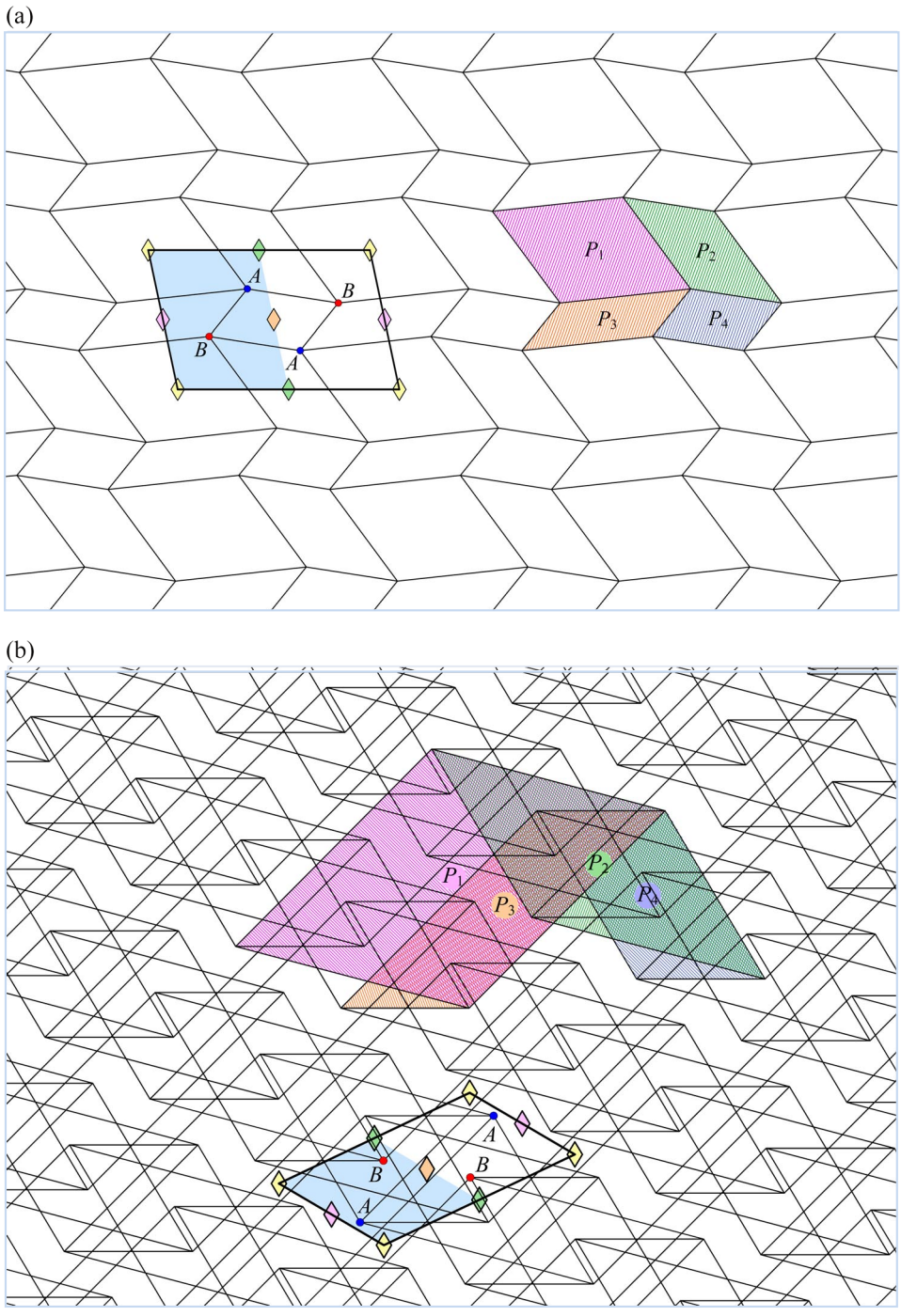

Figure 7. (a) An example for a flat-foldable $(p2)^{+}_{2,2}$ variation of the Miura-ori. The unit cell is depicted on the left. The unit fragment, which consists of four different starting parallelograms, shown as P_1, P_2, P_3 and P_4, is illustrated on the right; (b) a zoomed-in view of the pattern in the flat-folded condition along with its unit cell and the relative position of the starting parallelograms.

fragment consists of four different starting parallelograms, shown as P_1, P_2, P_3 and P_4. This figure reveals that the pattern is a $(p2)^{+}_{2,2}$ variation of the Miura-ori. A zoomed-in view of the pattern in its flat-folded condition is depicted in Figure 7.b, along with its unit cell and the relative position of the starting parallelograms. The folding process of this pattern can be thought of as a transformation of a $p2$

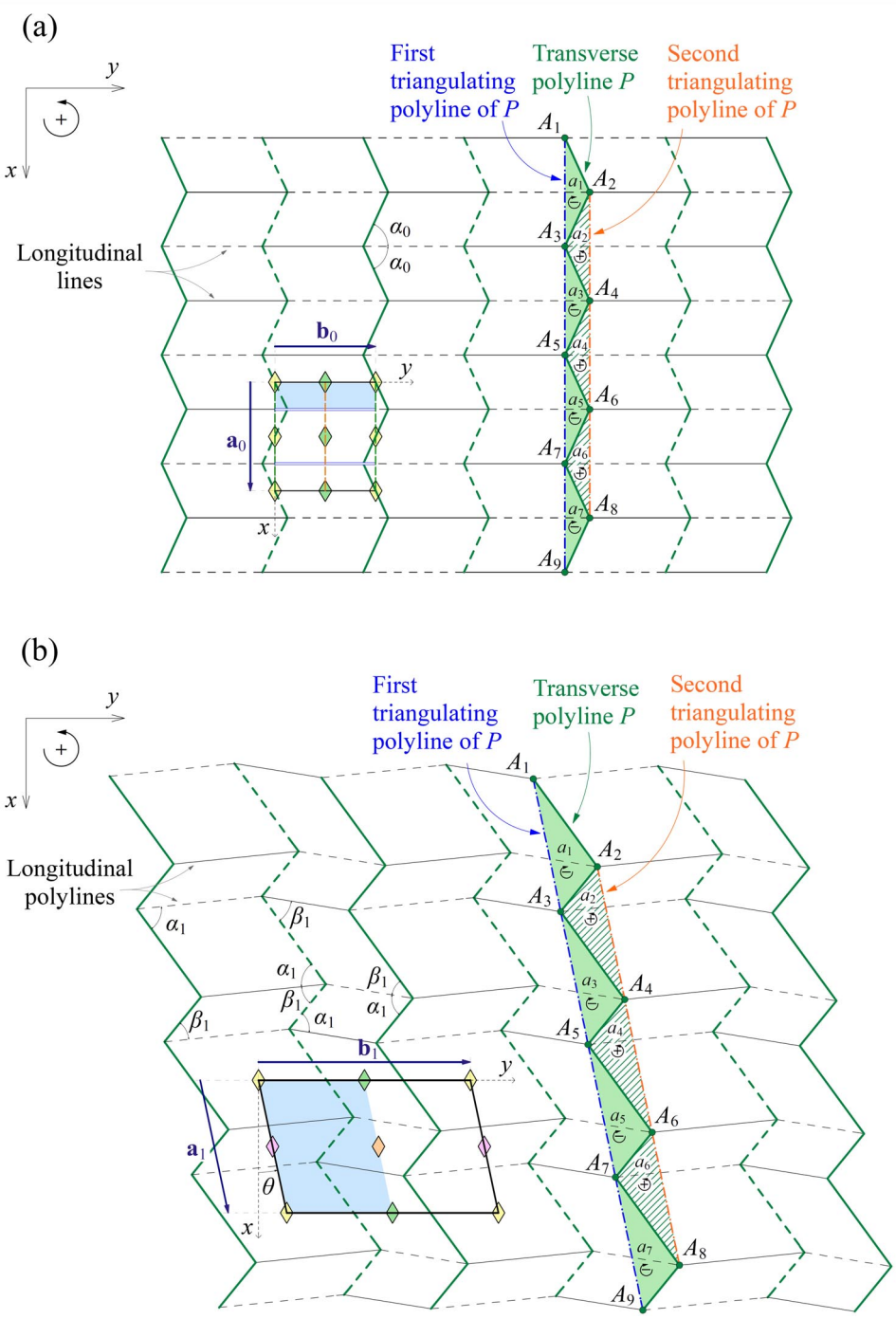

Figure 8. (a) A Miura fold pattern; (b) an inclined variation of the Miura fold pattern [2]. Mountain and valley folds are represented by solid and dashed lines, respectively. Transverse polylines are shown in bold green lines, while longitudinal lines (polylines) are in black. The blue and orange dot-dashed polylines corresponding to each transverse polyline illustrate its first and second triangulating polyline, respectively. The odd-numbered and even-numbered triangles formed by the triangulation are shaded and hatched, respectively. The unit cell of each pattern is shown on the bottom left of the figure. The blue shaded areas show the fundamental region of the patterns. Different colours for a symmetry element represent different classes of that element in the patterns.

wallpaper pattern, a $(p2)^{+}_{2,2}$ variation of the Miura-ori, into another $p2$ wallpaper pattern.

If a pattern is not globally planar, it will fold to a figure with an overall curvature which inevitably self-intersects for an infinite pattern. Such patterns are called *globally curved* patterns. An example for a globally curved pattern will be shown in Figure 14. It has been shown [13] that such patterns may fold to finite plane symmetry groups such as dihedral groups.

In the next section, we explore design variations on the Miura fold pattern systematically.

3. LEGITIMATE DESIGN VARIATIONS ON THE MIURA-ORI

3.1. Concepts and definitions

Consider the Miura-ori crease pattern shown in Figure 8.a alongside the depicted coordinate system. The orthogonal x-y-coordinate system remains a fixed reference as we vary the pattern, throughout this study. The horizontal fold lines are called the *longitudinal lines*. A longitudinal line, shown in black, consists of a number of fold line segments which alternate between mountain and valley. The rectangular unit cell of this pattern is shown on the bottom left of the figure.

In general, the longitudinal line segments do not lie on straight lines, but are the line segments of a set of polylines. The fold pattern in Figure 8.b [2] is an example for this type of variation of the Miura-ori. The parallelogram unit cell of this pattern is shown on the bottom left of the figure. The MARS fold pattern [14], which is perhaps the most well-known variation of the Miura-ori in which the longitudinal lines are replaced by piecewise parallel polylines, is a special case of the fold pattern in Figure 8.b when one of the fold angles, α_1 or β_1, is 90°. We call each of these polylines a *longitudinal polyline* of the fold pattern. The direction in which the longitudinal polylines travel is called the *longitudinal direction* of the pattern. In Figure 8, the y-axis is the longitudinal direction of the depicted fold patterns. Note that, in both cases, one of the translation vectors of the pattern ($\mathbf{b}_0$ in Figure 8.a, and $\mathbf{b}_1$ in Figure 8.b) is horizontal, i.e. parallel to the longitudinal direction.

Transverse to the longitudinal direction, there are zigzag polylines which are shown in green. The main characteristic of these polylines is that each of them is composed of line segments which all have the same mountain-valley assignment, while neighbouring polylines are alternately given a mountain then valley assignment. We call each of these polylines a *transverse polyline* of the fold pattern. The direction in which the transverse polylines travel is called the *transverse direction* of the pattern. In Figure 8, the x-axis is the transverse direction of the depicted fold patterns.

In the rest of this study, we investigate legitimate variations on the Miura-ori where we use the definitions above extensively.

3.2. Design variations

Assume we are given a Miura fold pattern, as shown in Figure 9.a. We consider moving nodes of the pattern, such as A and B, but require that the connectivity of the mesh is preserved, all line segments in the mesh remain straight, and that there is no crossing of the mesh lines. Figure 9.b shows a variation of the pattern shown in part (a) with two displaced nodes A' and B', while the other nodes have remained unchanged.

Based on this method of design variation, the following definition is our criteria to judge whether a variation on the Miura fold pattern is legitimate:

***Definition* 3:** A variation on a given Miura fold pattern is considered to be a *legitimate variation* if the following requirements are met:

i. All the facets remain convex quadrilaterals;
ii. The 'unidirectional chevron shape' of the Miura pattern is preserved (the global zigzag condition defined in Section 3.3).

Having satisfied the above requirements, the next step in designing a flat-foldable legitimate variation of the Miura-ori is to examine the possibility of satisfying the local flat-foldability condition at each node of the pattern. Condition (i) is necessary for the flat-foldability of a pattern. Condition (ii) uses the new concept of 'global zigzag'. The unidirectional chevron shape of the Miura crease pattern gives it a global 'stacking while folding' behaviour. We present a mathematical condition for this type of behaviour through the concept of global zigzag.

3.3. Global zigzag condition

The definition of a zigzag polyline – although it is very intuitive – is not well defined in the geometry literature. A definition is presented in Du, et al. (1983) for a specific purpose.

We introduce an alternative definition for a zigzag polyline based on a specific triangulation. Assume a simple (non-self-intersecting) polyline P connecting n vertices $A_1, A_2, A_3, ..., A_n$ as shown in Figure 10. We add a second polyline P_1, connecting the odd-numbered vertices of P, depicted by blue dot-dashed lines. Polyline P_1 forms a *partial alternating triangulation* of polyline P. This partial triangulation generates *odd-numbered*

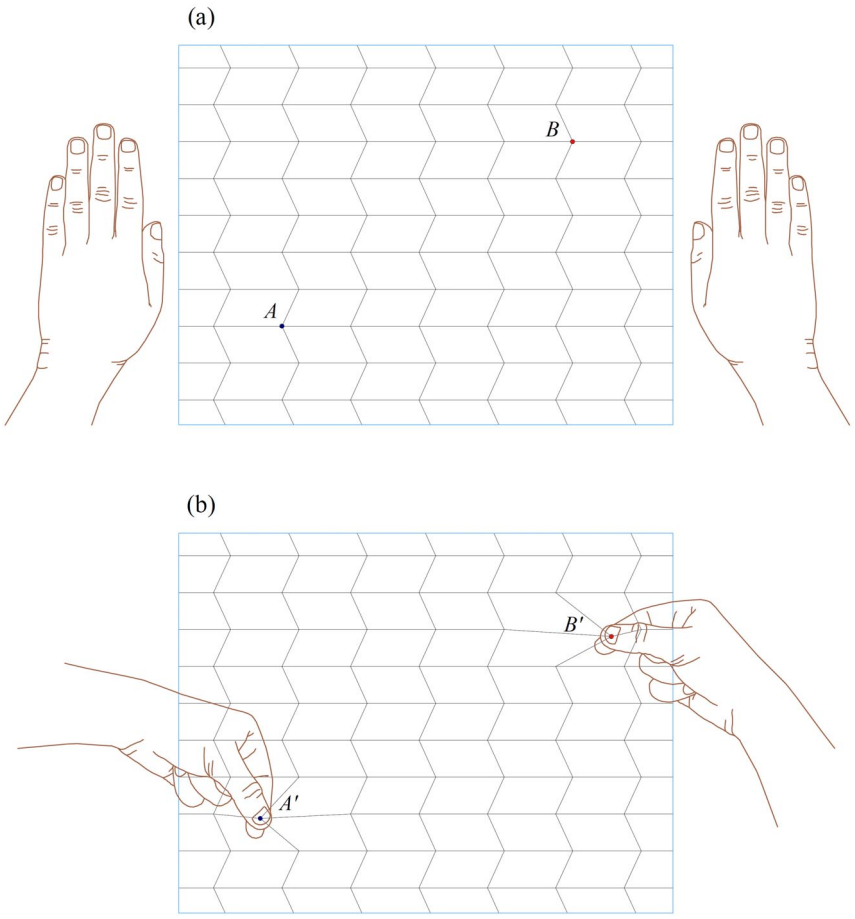

Figure 9. (a) A Miura fold pattern; (b) the Miura fold pattern shown in part (a) with two displaced nodes.

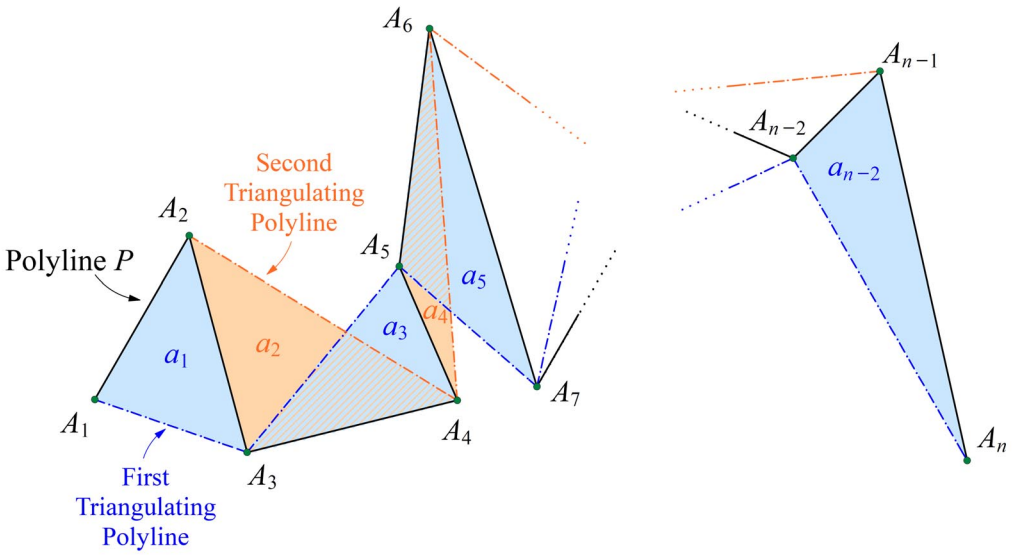

Figure 10. A polyline P connecting n vertices $A_1, A_2, A_3, \ldots, A_n$ is shown in black; its first and second triangulating polylines, P_1 and P_2, are depicted by blue and orange dot-dashed lines, respectively. Odd-numbered triangles, $a_1, a_3, \ldots$, and even-numbered triangles, $a_2, a_4, \ldots$, are shaded in blue and orange, respectively, having overlaps in the hatched regions.

triangles a_1, a_3, a_5, and so on, shaded in blue in the figure. We call P_1 the *first triangulating polyline* of P. Similarly, we add another polyline P_2 to the figure, connecting the even-numbered vertices of P, shown by orange dot-dashed lines. Polyline P_2 forms another partial alternating triangulation of polyline P. This partial triangulation generates *even-numbered triangles* a_2, a_4, a_6 and so on, shaded in orange in the

figure. We call P_2 the *second triangulating polyline* of P. Polylines P_1 and P_2 together form the *complete alternating triangulation* of polyline P.

***Definition* 4:** A simple polyline P, consisting of n vertices A_1, A_2, A_3, ... , A_n, where $n \geq 4$, is called *zigzag* if:

1) All odd-numbered triangles $A_i A_{i+1} A_{i+2}$, $i = 1, 3, \ldots, p$, where $p = n - 3$ for $n \geq 4$ even and $p = n - 2$ for $n \geq 5$ odd, are either clockwise, or all are counter-clockwise;
2) All even-numbered triangles $A_{i+1} A_{i+2} A_{i+3}$, $i = 1, 3, \ldots, q$, where $q = n - 3$ for $n \geq 4$ even and $q = n - 4$ for $n \geq 5$ odd, have a direction opposite to the direction of the odd-numbered triangles.

The triangulation above forms a total number of $n - 2$ triangles, which includes $(p + 1)/2$ odd-numbered triangles and $(q + 1)/2$ even-numbered triangles.

Now we have the tools to explain when the unidirectional chevron shape of the Miura fold pattern is preserved. In a legitimate variation of the Miura-ori, all transverse polylines must be zigzag, and pointing towards the same direction (i.e. corresponding triangles must have the same direction), when tracked starting from the same longitudinal line (polyline). We call this condition the *global zigzag condition* of the transverse polylines. Combining this condition with the local flat-foldability condition (opposite angles must sum to π) allows us to preserve a mapping between the mountain-valley assignment of the initial Miura-ori with the mountain-valley assignment of the descendant pattern, which guarantees the existence of a valid mountain-valley assignment for the descendant fold pattern. Here we show how the mapping is preserved.

The Miura fold pattern consists of only one node type which is flat-foldable for any fold angle α_0 ($\alpha_0 \neq 0$ or π). We call this node type a *mirror node*. A degree-4 node which is not a mirror node is called a *generic node*. Figure 11 shows a mirror node, B, versus a *generic node*, B'.

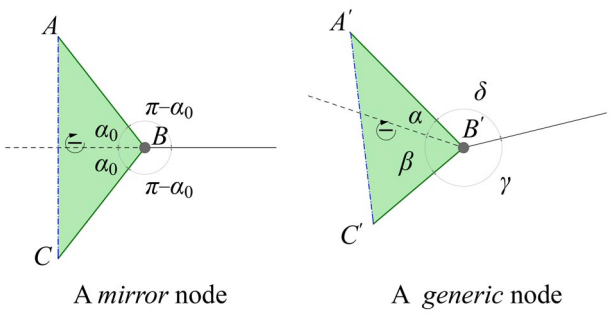

Figure 11. A mirror node versus a generic node; transverse polylines are shown in bold green lines, while longitudinal polylines are in black. Triangles formed by the triangulation of the transverse polylines are shaded in green.

Assume that a specific mirror node B, of a given Miura-ori, is deformed to a generic node B', such that triangles ABC and $A'B'C'$ are both clockwise. If B' is flat-foldable, we have

$$\alpha + \gamma = \beta + \delta = \pi \tag{3}$$

As triangle $A'B'C'$ is a clockwise triangle, we have

$$\alpha + \beta < \pi < \gamma + \delta \tag{4}$$

without loss of generality, we can assume $\alpha \leq \beta$. Combining this inequality with Equations (3) and Inequalities (4) gives us

$$\alpha < \gamma \tag{5}$$

In a similar way, we can show

$$\alpha < \delta \tag{6}$$

As a result, α is the (strictly) smallest angle among the four angles around node B'. On the other hand, we know that if a single vertex is locally flat-foldable, each angle which is strictly smaller than its two neighbouring angles has two opposite fold directions, i.e. one mountain and one valley (see [15]). Therefore, α is the angle with two opposite fold directions, which means that there is a mapping between the mountain-valley assignment of the initial mirror node B with the mountain-valley assignment of the generic node B'.

Referring back to Figure 8, the odd-numbered and even-numbered triangles formed by the complete alternating triangulation are shaded and hatched, respectively. There is only one type of transverse polyline in each fold pattern (a) or (b). Both patterns are globally zigzag, as all the shaded triangles are pointing clockwise.

A well-known example of a locally flat-foldable pattern which is not globally zigzag is the pattern shown in Figure 12. This is because of the fact that the even-numbered triangles associated with polyline P_a, the purple shaded triangles, are clockwise, whereas the even-numbered triangles associated with polyline P_b, the green shaded triangles, are counter clockwise. It should be noted that having alternating mountain-valley assignments for the transverse polylines is not possible in this pattern, since to preserve the local flat-foldability of each node in this case, all the transverse polylines should have the same mountain-valley assignment.

An interesting point is that, in general, the longitudinal polylines do not have to be zigzag. An example for this type of variations of the Miura-ori is depicted in Figure 13.

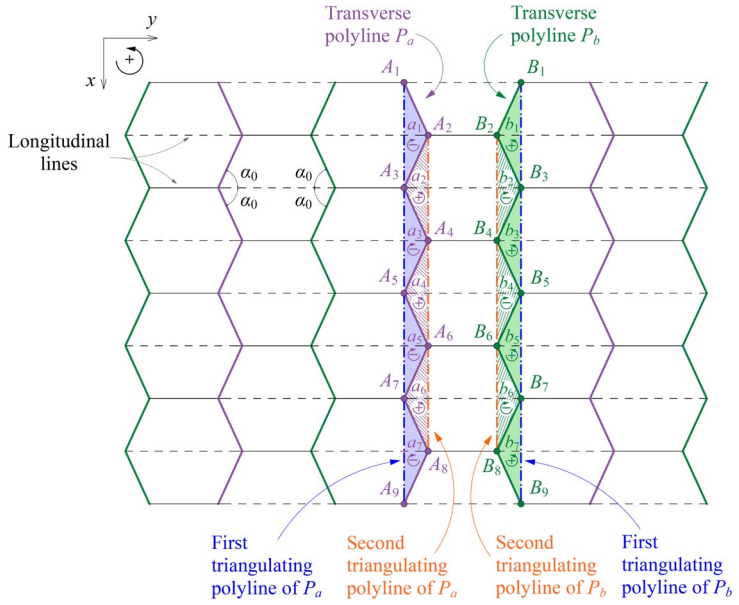

Figure 12. A cylindrical fold pattern [1] with the same nodal angle as in the Miura-ori in Figure 8.a; mountain and valley folds are represented by solid and dashed lines, respectively. The blue and orange dot-dashed polylines corresponding to each transverse polyline illustrate its first and second triangulating polyline, respectively. The odd-numbered and even-numbered triangles formed by the triangulation are shaded and hatched, respectively. The direction of each triangle is shown. There are two different types of transverse polylines, P_a and P_b.

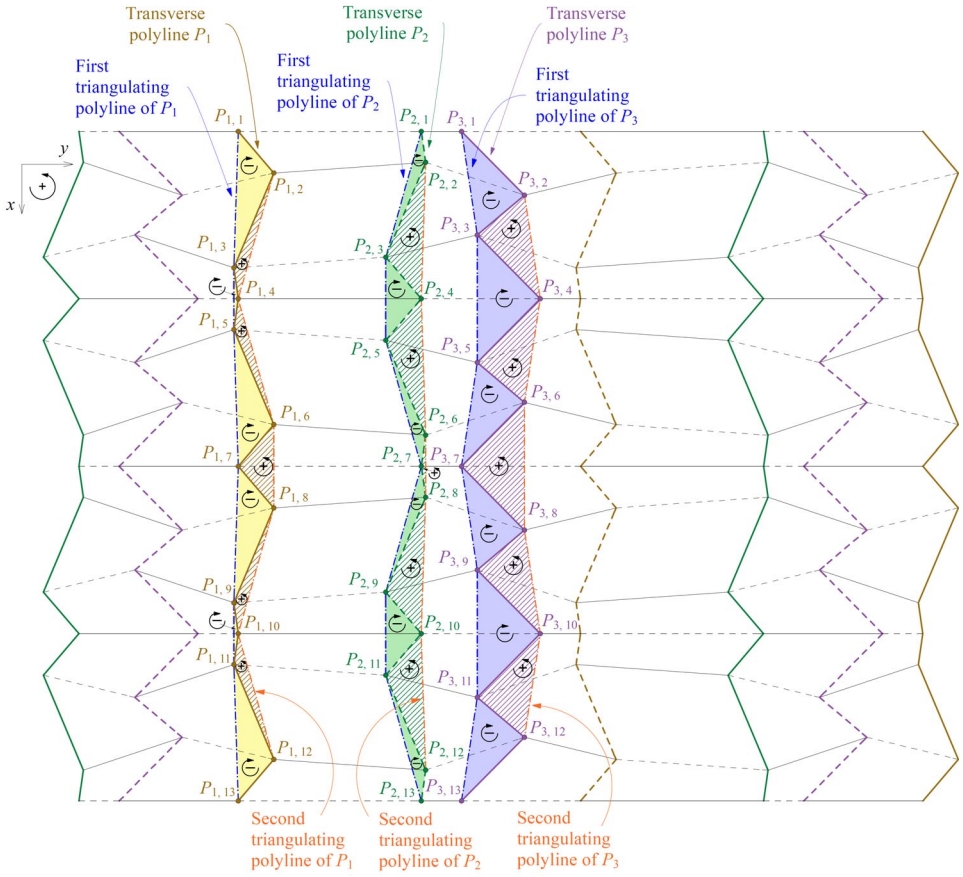

Figure 13. A legitimate variation of the Miura-ori; mountain and valley fold lines are represented by solid and dashed lines, respectively. The blue and orange dot-dashed polylines corresponding to each transverse polyline illustrate its first and second triangulating polyline, respectively. The odd-numbered and even-numbered triangles formed by the triangulation are shaded and hatched, respectively. The direction of each triangle is shown. There are three different types of transverse polylines in this pattern.

Definitions 1 through 4, along with the plane symmetry groups and the flat-foldability condition, are our mathematical tools in order to make consistent variations on the Miura fold pattern.

4. AN EXAMPLE OF RESULTS

Applying the proposed variations to the Miura-ori, we have developed an extensive family of derivatives for this pattern. The derivation of some of these variations has already been presented in [16] and [17]. More extensive details can be found in [18] and [19]. For the sake of brevity, we do not explain the design details here, but we only present an example fold pattern designed using the framework.

Figure 14 shows an example for a flat-foldable $pmg_{6,2}$ variation of the Miura fold pattern alongside the assigned mountains and valleys. The pattern consists of three different starting convex quadrilaterals, shown as Q_1, Q_2 and Q_3. The unit fragment of the pattern is shown on the right hand side of the crease pattern. The lower part of the figure shows a cardboard model of the fold pattern; the picture on the bottom right shows the model in its flat-folded condition. The other pictures show the model in

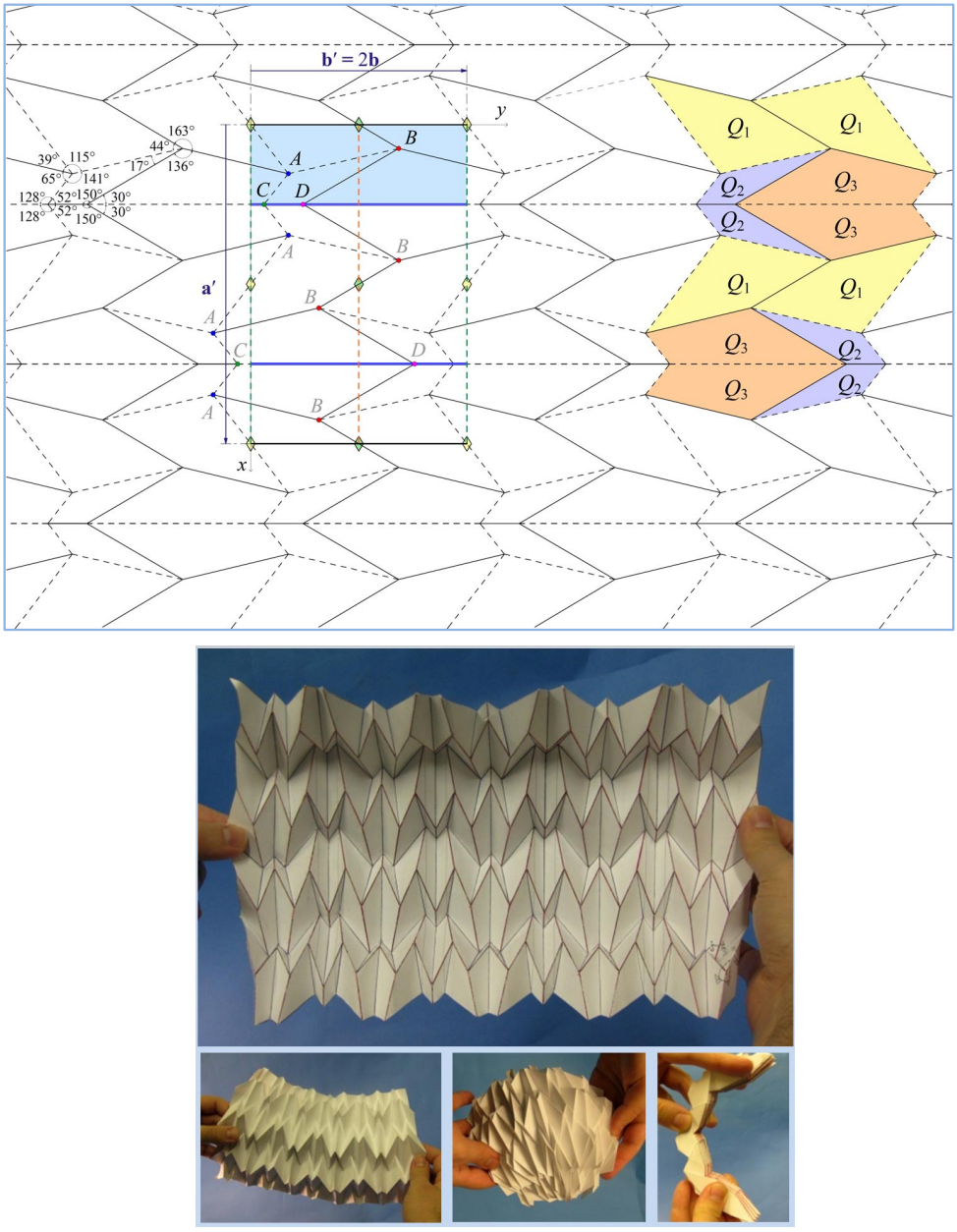

Figure 14. Top: an example for a flat-foldable $pmg_{6,2}$ variation of the Miura-ori. It consists of three different starting convex quadrilaterals, shown as Q_1, Q_2 and Q_3. Solid lines show mountain fold lines, while dashed lines represent valley fold lines; bottom: a cardboard model of the fold pattern depicted in the previous figure; the picture on the bottom right shows the model in its flat-folded condition. The other pictures show the model in a partially folded state, deformed or non-deformed.

a partially folded state, deformed or non-deformed. As we see in this figure, the model is globally curved in the *y*-direction.

5. CONCLUSIONS

We developed a framework for applying design variations on the Miura-ori, through which we presented a number of novel geometric concepts and definitions such as global planarity. We looked at the Miura-ori as a globally planar pattern based on a single starting parallelogram. Using wallpaper groups and subgroup relationships among them, we showed that through appropriate design variations on the original pattern, it can be used to systematically design flat-foldable tessellations with a variety of quadrilateral facets, which are either globally planar, or globally curved.

REFERENCES

[1] Nojima, Taketoshi. Modelling of Folding Patterns in Flat Membranes and Cylinders by Origami. *JSME International Journal Series C*, 45, 1 (2002), 364–370,

[2] Sareh, Pooya and Guest, Simon D. Tessellating Variations on the Miura Fold Pattern, (Seoul, South Korea 2012), IASS-APCS Symposium.

[3] Tachi, Tomohiro. Generalization of Rigid-Foldable Quadrilateral-Mesh Origami. (Valencia, Spain 2009), Proceedings of the International Association for Shell and Spatial Structures (IASS).

[4] Miura, Koryo, Map Fold a La Miura Style. Its Physical Characteristics and Application to the Space Science. *Research of Pattern Formation, edited by R. Takaki, © KTK Scientific Publishers* (1994), 77–90.

[5] O'Rourke, Joseph. *How to Fold It: The Mathematics of Linkages, Origami, and Polyhedra*. Cambridge University Press, 2011.

[6] Miura, Koryo. The Science of Miura-ori: A Review. In *Fourth International Conference on Origami in Science, Mathematics, and Education (4OSME)* (Pasadena, CA 2006), Fourth International Conference on Origami in Science, Mathematics, and Education (4OSME).

[7] Schwarzenberger, R. L. E. The 17 plane symmetry groups. *Mathematical Gazette 58* (1974), 123–131.

[8] Schattschneider, Doris. The Plane Symmetry Groups: Their Recognition and Notation. *The American Mathematical Monthly*, 85, 6 (Jun. – Jul., 1978 1978), 439–450.

[9] Hahn, Th. *International Tables for Crystallography, Volume A: Space-group symmetry*. Springer, USA, 2005.

[10] Radaelli, Paolo G. *Symmetry in Crystallography: Understanding the International Tables*. Oxford University Press, 2011.

[11] Senechal, Marjorie. Point groups and color symmetry. *Zeitschrift für Kristallographie - Crystalline Materials*, 142, 1–2 (1975), 1–23.

[12] Jablan, Slavik. *Theory of Symmetry and Ornament*. Matematicki Institut, Yugoslavia, 1995.

[13] Sareh, Pooya. Symmetric Descendants of the Miura-ori. *PhD Dissertation, Engineering Department, University of Cambridge, UT* (2014).

[14] Barreto, P. T. Lines meeting on a surface: The "Mars" paperfolding. (Otsu, Japan 1997), Origami Science & Art: Proceedings of the Second International Meeting of Origami Science and Scientific Origami (1997), 343–359.

[15] Demaine, Erik D and O'Rourke, Joseph. *Geometric Folding Algorithms: Linkages, Origami, Polyhedra*. Cambridge University Press, 2007.

[16] Sareh, Pooya and Guest, Simon D. Minimal Isomorphic Symmetric Variations on the Miura Fold Pattern. (Seville, Spain 2013), The First International Conference on Transformable Architecture (Transformable 2013).

[17] Sareh, Pooya and Guest, Simon D. Designing Symmetric Derivatives of the Miura-ori. (London 2014), Advances in Architectural Geometry 2014.

[18] Sareh, Pooya and Guest, Simon D. Design of Isomorphic Symmetric Descendants of the Miura-ori. *Smart Materials and Structures* (2015).

[19] Sareh, Pooya and Guest, Simon D. Design of Non-isomorphic Symmetric Descendants of the Miura-ori. *Smart Materials and Structures* (2015).